

# AhaRobot: A Low-Cost Open-Source Bimanual Mobile Manipulator for Embodied AI

Haiqin Cui<sup>\*,1</sup>, Yifu Yuan<sup>\*,1</sup>, Yan Zheng<sup>1</sup>, Jianye Hao<sup>1</sup>

**Abstract**—Navigation and manipulation in open-world environments remain unsolved challenges in the Embodied AI. The high cost of commercial mobile manipulation robots significantly limits research in real-world scenes. To address this issue, we propose *AhaRobot*, a low-cost and fully open-source dual-arm mobile manipulation robot system with a hardware cost of only \$1,000 (excluding optional computational resources), which is less than 1/15 of the cost of popular mobile robots. The *AhaRobot* system consists of three components: (1) a novel low-cost hardware architecture primarily composed of off-the-shelf components, (2) an optimized control solution to enhance operational precision integrating dual-motor backlash control and static friction compensation, and (3) a simple remote teleoperation method *RoboPilot*. We use handles to control the dual arms and pedals for whole-body movement. The teleoperation process is low-burden and easy to operate, much like piloting. *RoboPilot* is designed for remote data collection in embodied scenarios. Experimental results demonstrate that *RoboPilot* significantly enhances data collection efficiency in complex manipulation tasks, achieving a 30% increase compared to methods using 3D mouse and leader-follower systems. It also excels at completing extremely long-horizon tasks in one go. Furthermore, *AhaRobot* can be used to learn end-to-end policies and autonomously perform complex manipulation tasks, such as pen insertion and cleaning up the floor. We aim to build an affordable yet powerful platform to promote the development of embodied tasks on real devices, advancing more robust and reliable embodied AI. All hardware and software systems are available at <https://aha-robot.github.io>.

## I. INTRODUCTION

Recent advances in robotic manipulation [1], [2], [3], [4], [5] and navigation [6], [7], [8] have shown significant progress in embodied AI. Many tasks in everyday environments, such as cooking and house cleaning, require coordination of the entire body and dexterous use of dual arms. Therefore, bimanual mobile manipulators have been widely applied in embodied tasks [9], [10]. However, previous research hardware faced two issues: *high cost* and *limited operational space*. Bimanual mobile robots are generally expensive and difficult for research laboratories to afford, with an average cost of \$30,000, posing a major barrier for researchers entering this field. Some hardware platforms are limited to desktop operations or may lack sufficient workspace (e.g. reaching the ground), which poses new challenges for deploying them in everyday environments.

Using bimanual mobile robots for Imitation Learning also raises higher requirements for teleoperation data collection. Human operators must simultaneously control both arms

and maneuver the entire body for complex, long-horizon tasks across various scenarios, surpassing the complexity of desktop operations. A popular approach is the visual scheme, such as using Virtual Reality (VR) devices [11], [12], [13]. This solution requires an investment in VR equipment, and the weight of the devices makes them unsuitable for long-term remote operation. It also necessitates additional adaptation of base controllers to achieve complete control of mobile robots. Using two 3D mice [14] or joysticks is a similar alternative, but it struggles with whole-body remote operation. Another approach is the leader-follower scheme [9], [1], [15], [16], [17], [18], which involves constructing an additional arm with the same joint configuration as the target robotic arm to capture joint angle data, requiring additional motors or encoders. However, works like Mobile Aloha typically require manual operation of the machine, cannot be remotely controlled, and face difficulties when dealing with extremely long-distance operations.

To address the issue, we introduce *AhaRobot*, a low-cost open-source bimanual mobile manipulator within a base budget of \$1,000. *AhaRobot* can be configured with different specifications of computing resources to support tasks with varying computational requirements. Our design focuses on several key concepts: the affordability of the entire system, support for whole-body mobility, and the ability to operate at various heights. Additionally, it ensures the precision required for completing daily tasks while providing user-friendly and low-burden teleoperation methods to facilitate data collection. As shown in Table I, compared to other popular robotic arm platforms, *AhaRobot* can cover comprehensive operating functions and workspace, while its price is only 1/15. We present the core configuration and system of *AhaRobot* in Fig. 1. *AhaRobot* consists of three parts: ① *Hardware Configuration*: We propose a novel low-cost robot configuration, entirely based on off-the-shelf components. We use a sliding rail to replace the shoulder joint, avoiding the need for high-torque motors to counteract gravity. The *AhaRobot* is equipped with flexible dual-arm manipulation, full-body movement capabilities, and the ability to reach the floor. ② *Control System*: To meet the accuracy requirements of daily manipulation with a low-cost configuration, we optimize the control system of the *AhaRobot*. We introduce a dual-motor anti-backlash control method and static friction compensation, which significantly reduces the *AhaRobot*'s jitter and improves the trajectory tracking accuracy during task execution. ③ *Teleoperation*: Additionally, we propose *RoboPilot* teleoperation, enabling the operation of high degree-of-freedom dual-arm mobile

\*Equal Contributions

<sup>1</sup>College of Intelligence and Computing, Tianjin University, China  
{cuihaiqin, yuanyf, yanzheng, jianye.hao}@tju.edu.cn

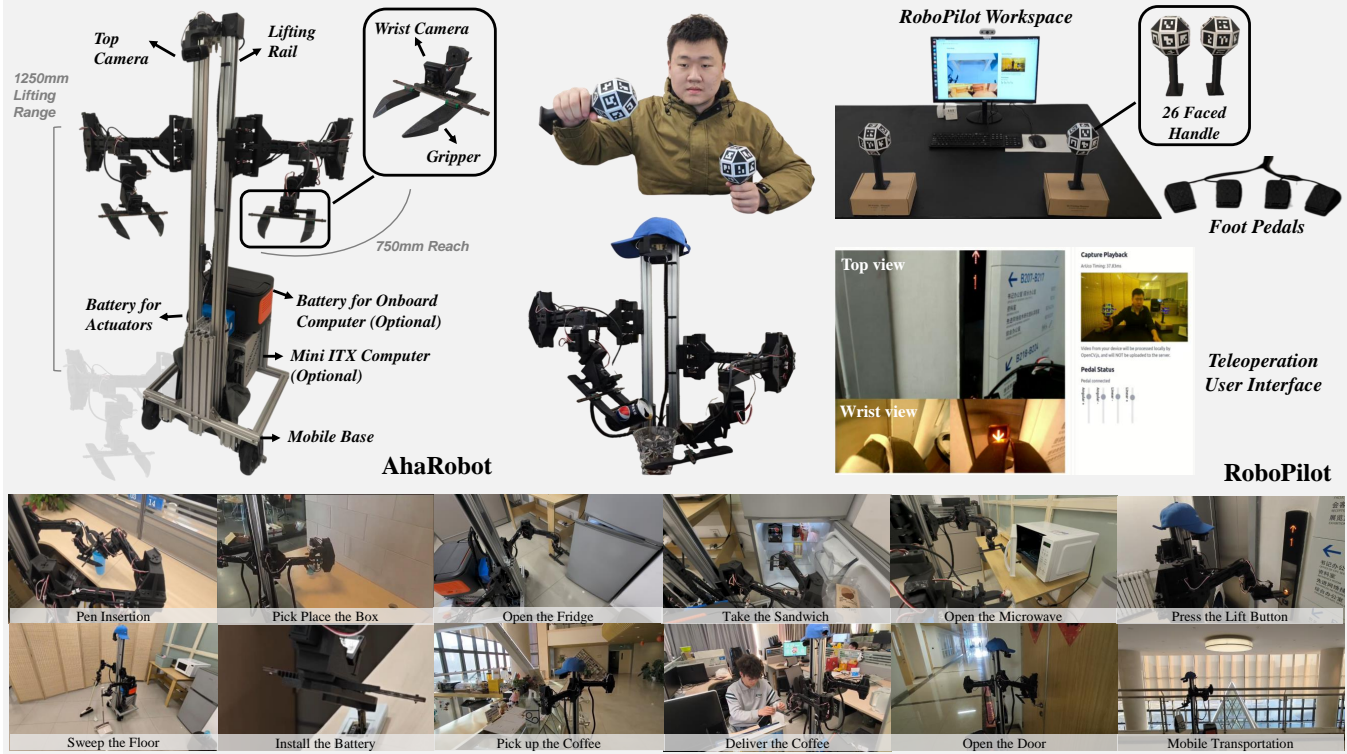


Fig. 1: **Overview of AhaRobot.** The system costs only \$1,000 for the robot and \$1,000 for extra power and computing. *Above left:* Hardware Configuration of AhaRobot. *Above right:* Fully Remote Mobile Manipulation Teleoperation RoboPilot. *Below:* AhaRobot can perform various tasks in daily life.

robots as easily as piloting. We first design a 26-faced marker handle for controlling the robot arms to mitigate the pose ambiguity problem and ultimately achieve a teleoperation precision of 3mm. Subsequently, several foot pedals are used to control the gripper, robot upper limb height, and whole-body movement. The human operator remotely intervenes through an interface that provides a view from the robot. RoboPilot can be easily integrated into various types of robots. RoboPilot only requires a cost of \$50, whereas the similar teleoperation solutions of Mobile Aloha [9] and BiDex [18] require \$7,200 and \$6,395 respectively. Additionally, RoboPilot can be fully remotely operated, unlocking the potential for large-scale crowdsourced data collection. We evaluated this robot on multiple household tasks, and the experimental results demonstrate that our robot meets the demands of real-world application. We conducted extensive experiments in real-world scenarios, including the ablation of various components, comparison of the efficiency of teleoperation in complex tasks, and imitation learning experiments, all of which demonstrated that the AhaRobot can meet the application requirements of real-life application and become a hardware foundation for Embodied AI.

Our contributions can be summarized as follows: 1) **AhaRobot Design:** We propose a novel robot design capable of dual-arm coordination, providing freedom of lifting, and aligning with human dimensions. Furthermore, we enable the robot to achieve the precision necessary for daily tasks with low-cost components by control system optimization. The entire robot is designed within a budget of \$1000 (without

TABLE I: **Comparison of Different Robotic Platform.** †: The price of \$1000 does not include computing resources, while \$2000 version is for the Mini-ITX computer with an RTX4060 GPU.

Robot Platform	Cost	Dual Arm	Mobile Base	Reach Floor	Hardware Open-Source	DoF
Mobile Aloha [9]	\$32,000	✓	✓	✗	✓	16
Hello Robot [19]	\$24,950	✗	✓	✓	✗	7
DROID [20]	≈ \$27,000	✗	✗	✗	✗	8
AgileX COBOT	≈ \$30,000	✓	✓	✗	✗	16
TIAGo	> \$200,000	✗	✓	✗	✗	11
<b>AhaRobot<sup>†</sup></b>	<b>\$1,000-2,000</b>	<b>✓</b>	<b>✓</b>	<b>✓</b>	<b>✓</b>	<b>16</b>

computational resources) to \$2,000 (Mini-ITX computer with RTX4060 GPU), only 1/15 of the popular mobile robotics platforms, offering a cost-effective solution for real-world settings. 2) **RoboPilot Teleoperation Method:** We implement a teleoperation system based on 26-faced fiducial markers and foot pedals for \$50, achieving a teleoperation precision of 3mm. The operator interacts with the robot through a web-based interface to achieve fully remote teleoperation. 3) **Open-Source Hardware & Software:** To promote openness and sharing in the robotics community and reduce the costs for researchers in real-world experiments, we have fully open-sourced the hardware and software designs of the robot configuration and teleoperation system. Users can easily start the entire robot by following the installation guide.

## II. RELATED WORKS

**Mobile Manipulator:** Mobile manipulation robots are capable of whole-body coordinated mobility and dexterous manipulation [9]. One common method for constructing a mobile manipulator is to mount an industrial robotic arm on a mobile base [21], [18], [22], [19], [23], [24]. Some research [25], [26], [27] suggests replacing the base with a quadrupedal robot to enhance terrain adaptability. However, these designs often struggle with limited lifting freedom and dual-arm coordination, resulting in a constrained working area. Several efforts [28], [29], [30], [31], [19] focus on developing new robotic configurations from scratch to overcome these challenges. These typically involve multiple custom components and are costly, making future enhancements difficult. AhaRobot utilizes off-the-shelf components with low-cost configurations. Also, users can easily begin experiments with an identical robot setup as AhaRobot with a fully open-source installation guide.

**Teleoperation:** Learning-based methods [1], [2], [32], [33], [3] have been widely applied to mobile manipulation, making the efficient collection of human demonstration crucial. A common type of teleoperation method [11], [12], [13], [34] uses vision-based methods like Virtual Reality (VR) devices to capture the pose of end-effectors. However, this method requires the teleoperator to wear heavy VR equipment, making it unsuitable for long-term teleoperation. Similarly, other vision-based methods utilizing human motion capture suits [35], [36] demand significant investment in hardware. UMI family works [37], [38] design a low-cost gripper combined with SLAM to achieve results, yet SLAM may encounter localization failures and exhibit high latency, making it unsuitable for real-time remote operations. Another mainstream solution [16], [17], [1], [9], [15], [18] builds their exoskeleton-like teleoperation systems that rely on joint-to-joint control or inverse kinematics to retarget the teleoperator's movements to the robot arms. However, these systems often require additional electronic components and involve extensive manual assembly and wiring, making them difficult to set up. Additionally, most of these methods focus on upper-body teleoperation, leaving the integration of manipulation with mobile bases underexplored. For example, some solutions [9] require the teleoperator to manually push the robot for mobility, which is labor-intensive, while others rely on a second operator [15] to control the robot's base. This work focuses on achieving a low-cost, easy-to-build, and low-burden teleoperation method by utilizing a novel handle with 26-faced markers and a well-designed web-based teleoperation interface.

## III. LOW-COST AHAROBOT HARDWARE SYSTEM

We develop **AhaRobot**, a low-cost hardware system tailored for real-world application and seamless integration into domestic and office environments to perform common human tasks. The design adheres to four key requirements: 1) **Affordability:** The robot's configuration and component selection should be optimized for cost efficiency; 2) **Whole-Body Mobility:** Navigate different locations and execute

tasks at various heights; 3) **Minimal Footprint:** Compact design to facilitate movement through confined spaces; 4)

**Without On-site Assistance:** Recover from failures fully remotely.

*a) Morphology:* A well-designed mechanical structure is crucial for cost-effective task completion. As illustrated in Fig. 1, the robot features lifting rails supporting its upper body, SCARA-like arms with dexterous wrists, and a differential-drive mobile base.

**Lifting Capability:** Empirical evaluation of structures similar to Mobile Aloha revealed that the absence of lifting freedom often leads to irrecoverable failures, such as objects slipping from the robot's grasp. These failures typically necessitate on-site human intervention. To address this limitation (*requirement 2 and 4*), we incorporated lifting degrees of freedom into AhaRobot. While lead screws excel in precision positioning and load capacity, their limited movement speed makes them unsuitable for dynamic tasks. Instead, we adopted a belt-driven slide, which also serves as the robot's upper body.

**SCARA-like Arms:** The primary challenge in enhancing the load and operational range of robotic arms lies in the high inertia and gravitational loads, which demand greater torque density at the shoulder and elbow joints. To mitigate these challenges, we implemented a horizontal arm configuration. This design, in combination with the lifting mechanism described earlier, minimizes the impact of gravity on the joints, thus reducing the cost (*requirement 1*) and simplifying the control algorithms. Furthermore, the horizontal arm configuration allows the arms to fold and retract to the body during standby or moving, achieving minimal space occupation as mentioned in *requirement 3*.

**Dual-Motor Joints:** Inspired by the biomechanics of human joints [39], which rely on two sets of muscles to achieve zero-backlash movement, we developed a dual-motor setting. The joints are powered by low-cost Feetech STS3215 motors at the price of \$15 (*requirement 1*), which feature high-speed DC motors paired with a gearbox offering a 1:345 gear ratio and a maximum torque of 35 kg·cm. A modular design was adopted, facilitating easy repair. By applying appropriate bias tension through two servos in the control algorithm, the robotic arm achieves higher precision.

**Differential Drive Mobile Base:** Considering *requirement 2*, the robot employs a dual-wheel differential drive base. Two BLDC motors are installed at the front of the robot, while a universal wheel at the rear, providing in-place rotation (*requirement 3*). The base is constructed using aluminum profiles to securely attach the robot body, avoiding the high costs of CNC manufacturing or casting (*requirement 1*). Additionally, the front-to-back distance of the chassis has been minimized, limiting the sweeping area to a radius of 50 cm and reducing the risk of collisions during turns.

*b) Sensing:* The robot is equipped with three cameras: one mounted on the top of its head, providing a panoramic view of the environment, and two mounted on the left and right wrists, offering information for object approach and grasping. All cameras operate at a resolution of 640×360 and

a frame rate of 30 Hz. Furthermore, teleoperation at varying heights requires adaptable camera perspectives. To address these challenges, a 2-DoF pan-tilt gimbal was installed on the robot's head, enabling a wide and adjustable field of view. For proprioceptive sensing, each joint incorporates high-precision magnetic encoders with 4096 counts per revolution resolution. The base motors are equipped with Hall-effect position sensors with a resolution of 64 counts per revolution. Additionally, a photoelectric switch is installed at the bottom of the lifting slider to reset its position after power-on initialization or step losses in the stepper motors.

*c) Computing and Powering:* To achieve end-to-end automated manipulation and support model inference offline, AhaRobot is equipped with high-specification computational resources. It features a \$800 Mini-ITX-sized computer equipped with an Intel i5-12700KF CPU and an NVIDIA RTX4060 GPU. In many tasks, we can easily replace it with a cheaper onboard chip, such as NVIDIA Jetson Orin, to further reduce costs. Five ESP32 microcontroller modules are integrated to manage motion planning (acceleration/deceleration profiles) and PID control for the motors on the head, arms, and lift slider. An ODrive 3.6 controller is installed in the base to control the two BLDC motors. The robot operates on the ROS 2 Humble system, facilitating communication between different modules. The ESP32 and ODrive communicate with the computer via USB-TTL and USB-CAN, respectively. The robot is powered by a 20 Ah/24 V (294 Wh) lithium-polymer battery to supply power to the actuators. Additionally, a 1 kWh 220 V Jackery outdoor power supply is used to power the computer, enabling untethered operation. To balance the robot, both the computing and power modules are mounted at the rear of the robot. Safety features include an emergency stop mechanism for immediate system shutdown.

AhaRobot maximizes the use of off-the-shelf components, making it cost-efficient while delivering strong performance. The core parameters are as follows:

TABLE II: Core Parameters of AhaRobot

Category	Value
Payload (Single Arm)	1.5 kg
Weight	51 kg
Size	550*500*1550 mm
Max Gripper Width	120 mm
Max Reach (X-Y Plane)	750 mm
Z-Axis Reach	1250 mm
Battery Life	4-5 hr
Min Turning Radius	0
Truning Sweeping Radius	500 mm

#### IV. DUAL-JOINT CONTROL

The adaptation of low-cost components can result in manufacturing precision falling below expectations. Moreover, the high reduction ratio and brushed design of these motors lead to significant friction. These limitations impede the precise control of the robotic arm's end-effector, preventing the robot from completing delicate tasks. To mitigate

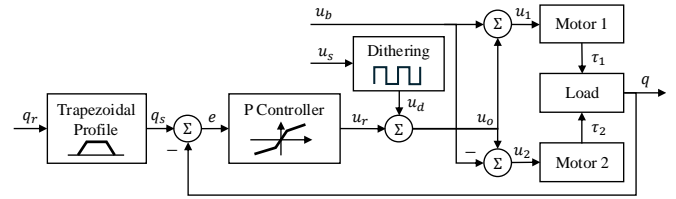
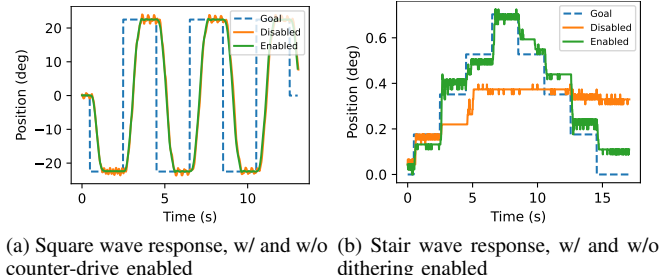


Fig. 2: Block Diagram of Dual-Joint Control System.



(a) Square wave response, w/ and w/o counter-drive enabled  
(b) Stair wave response, w/ and w/o dithering enabled

Fig. 3: System Responses with Different Control Strategies.

these limitations, we developed a dual-motor cooperative control method. Our method integrates dual-motor counter-drive backlash control and static friction compensation. The system's control block diagram is presented in Fig. 2.

#### Dual-Motor Counter-Drive Backlash Elimination:

Gear-based transmission reduction systems are often affected by backlash due to manufacturing constraints. Backlash introduces lag during gear direction switching, which significantly reduces the system's positioning accuracy. Under high-gain conditions, this lag can cause system oscillations, further compromising performance. We propose a method where the output shafts of two motors are directly connected, and a bias torque is applied to each motor. By engaging the motors with opposite gear faces, this approach effectively eliminates backlash. Additionally, a feed-forward backlash bias voltage term  $u_b$  is incorporated into the control loop to further improve system stability and performance:

$$\begin{cases} u_1 = u_o + u_b \\ u_2 = u_o - u_b \end{cases} \quad (1)$$

We compared the performance of enabling and disabling the module. The results (Fig. 3a) illustrate the tracking of a square wave target by recording the actual positions reported by the position sensor installed on the motor. When the counter-drive backlash elimination module is disabled, the joint exhibits oscillations around the target point due to the presence of backlash. This method successfully suppresses oscillations, which enhances positioning accuracy.

**Stiction Compensation through Motor Dithering:** The friction model, combining both Coulomb and viscous elements, is described by the following equation [40]:

$$\tau_f = \begin{cases} \tau_s \text{sgn}(\dot{q}) + \tau_v \dot{q}, & \text{if } \dot{q} \neq 0 \\ \tau_e, & \text{if } \dot{q} = 0 \text{ and } |\tau_e| < \tau_s \\ \tau_s \text{sgn}(\tau_e), & \text{otherwise} \end{cases} \quad (2)$$

where  $\tau_s$  denotes the maximum Coulomb friction;  $\tau_v$  represents the viscous friction coefficient;  $\tau_e$  signifies the external

torque, and  $q$  indicates the angle. Initial rotation necessitates overcoming the static threshold  $\tau_s$ . Low-cost motors typically exhibit higher  $\tau_s$ , resulting in the controller's incapacity to generate sufficient torque for motor actuation when position error remains minimal, thereby inducing persistent steady-state error.

A common approach to mitigate this issue is to introduce an integral controller. However, the accumulation of the integral term requires time, and due to constraints such as communication time, our frequency of the PID control cycle is relatively low (66 Hz). So, we introduce a simple technique by adding a feed-forward term  $u_d = (-1)^{\lfloor t/T \rfloor} u_b$  to the output, where  $T$  represents the cycle time of the PID loop, and  $u_b$  is the feed-forward term set to maintain the motor in a near-threshold state.

We conducted ablation experiments using micromotion tracking capabilities, employing a staircase trajectory with incremental steps of 0.175 degrees—twice the motor's minimum resolution. The results (Fig. 3b) showed that with motor dithering enabled, the system successfully tracked incremental target adjustments, whereas the control group with motor dithering disabled failed to follow the target.

## V. ROBOPILOT TELEOPERATION

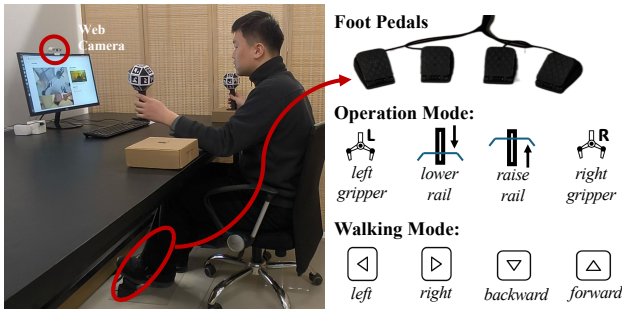


**Fig. 4: RoboPilot Teleoperation Workstation.** By capturing the 6D pose of the handle through a web camera, we can fully remotely teleoperate the robot, with the entire setup costing no more than \$50. Foot pedals can switch between two modes, respectively controlling the base's movement and the upper limbs' operation.

It is essential to develop a simple and useful teleoperation method for Embodied AI. We aim to design a teleoperation system for dual-arm mobile robots that is simple to construct, cost-effective, and sufficiently accurate while supporting fully remote operation—realizing the vision that “everyone can teleoperate a robot, just on their dining table” and unlocking the potential for data crowdsourcing to alleviate the data scarcity problem in embodied AI. We propose RoboPilot, a system comprising two passive handles, four Hall-effect pedals, a camera, and an ESP32 microcontroller. The construction cost for a single workstation is only \$50, and the system removes the need for bulky head-mounted displays, allowing for long-duration and fully remote teleoperation. A typical teleoperation workstation is shown in Fig. 4. The two handles capture the 6-DoF poses of the operator's left and

right hands, which are then retargeted to the end-effectors of the robotic arms via inverse kinematics. The four Hall-effect pedals control the movement of the robot's base, the opening and closing of the left and right grippers, and the large-scale movement of the lifting slider.

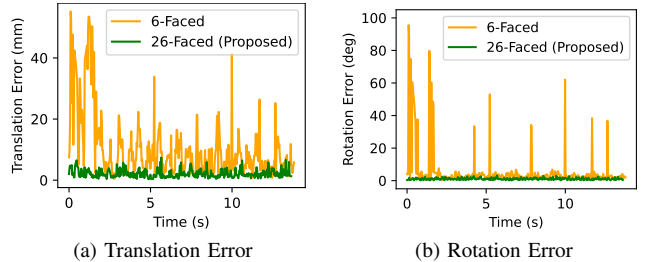


Fig. 5: Tracking Accuracy of Different Handles.

TABLE III: Quantitative Comparisons on Polyhedrons.

Type	Avg. Rotation Err	Avg. Translation Err
6-Faced	5.391 deg	9.9 mm
26-Faced (Ours)	1.094 deg ↓ (80%)	2.1 mm ↓ (79%)

**26-Faced Motion Capture Handle:** We use AprilTag [41] to capture the 6-DoF pose of the handle. A common method is to construct a 6-faced cube, but the perspective-n-point (PnP) algorithm with coplanar points exhibits pose ambiguity [42], particularly when the markers are parallel to the camera plane. This issue causes spikes in the estimated rotation, leading to low accuracy. To address this limitation, we designed a new marker configuration using a 26-faced polyhedron. When oriented toward the camera, multiple markers occupy non-coplanar positions, ensuring that the camera can detect at least three non-coplanar tags simultaneously from any viewpoint. We positioned our tag on a rotating platform and performed three complete rotations. Then, we measured both positional and rotational errors. As shown in Fig. 5, experimental results demonstrate that our 26-faced polyhedron significantly outperforms the conventional 6-faced cube, reducing the rotational error by 80% and the translational error by 79%, achieving an average positional accuracy of 3 mm.

**Pedals for Movement:** We employed four Hall-effect pedals to capture pedal press data. The pedals support two modes: walking mode and operation mode. Mode switching is controlled via keyboard shortcuts, with the pedals serving dual functions across the two modes. Detail functions are shown in Fig. 4. To ensure stable object gripping during base movement, the gripper's position can be locked using a designated keyboard key.

**Web-based Teleoperation Interface:** We developed a web-based teleoperation client for the operator. The capture and pose estimation of the 26-faced polyhedron are processed entirely on the client side using WebAssembly and OpenCV.js, ensuring the operator's privacy and data security. The four pedals transmit data via WebSerial, facilitated by an



**Task 1: Complete process of delivering coffee.** #Init AhaRobot departs from the laboratory on the 2<sup>nd</sup> floor #2-3 Passes through a long corridor and a corner #4-5 Aharobot retrieves coffee #6-8 Heads to the elevator, presses the button, and takes the elevator #9 Arrives at the target room on the 3<sup>th</sup> floor and opens the door #10 Successfully delivers the coffee.



**Task 2: Complete process of picking and heating sushi.** #Init AhaRobot are in front of the table #2-4 AhaRobot lowers its height and opens the lower refrigerator door #5 grabs the sushi from the refrigerator #6 moves and ascends to prepare for operating the microwave on the table, #7-8 uses both hands cooperatively to open the microwave and place the sushi inside, #9 closes the microwave, #10 descends and closes the refrigerator.

Fig. 6: **Very Long-horizon Remote Teleoperation.** We used RoboPilot to control AhaRobot and demonstrated two specially designed complex tasks. *Task 1* involves a very long sequence of operations with a total movement distance exceeding 200m, requiring remote tele-communication, agile movement, and precise environmental interaction. *Task 2* specifically showcases AhaRobot’s lifting and lowering capabilities, enabling it to touch the ground and complete more complex tasks in everyday life. We also demonstrated AhaRobot’s bimanual coordination by opening a microwave and placing sushi inside.

ESP32 microcontroller. The keyboard is used to issue specific commands, such as resetting the robotic arm’s position, switching the pedal mode, or locking the gripper. Video streams from the robot’s three cameras are transmitted to the web interface via WebRTC, while the handle’s 6-DoF pose data, along with keyboard and pedal inputs, are sent back to the robot through the WebRTC DataChannel.

## VI. EXPERIMENT

We conducted more experiments to verify the overall performance of AhaRobot and RoboPilot. 1) Is the RoboPilot convenient and user-friendly compared to other popular teleoperation solutions? 2) Can the combination of AhaRobot and RoboPilot achieve complex and long-horizon tasks? 3) Can AhaRobot achieve autonomous execution of mobility and manipulation tasks after imitation learning?

### A. Comparison of Teleoperation Solution

We compared RoboPilot with two commonly used approaches: Leader-Follower [9] and SpaceMouse [14]. For the leader-follower method, we utilized an early design prototype robotic arm. The SpaceMouse was configured to track the end-effectors pose’s position and rotation changes relative to the AhaRobot’s Base Frame. To ensure fair comparison, teleoperators were required to operate while seated at a computer and observed remotely images. Each participant had one warm-up opportunity, followed by the formal experiment,

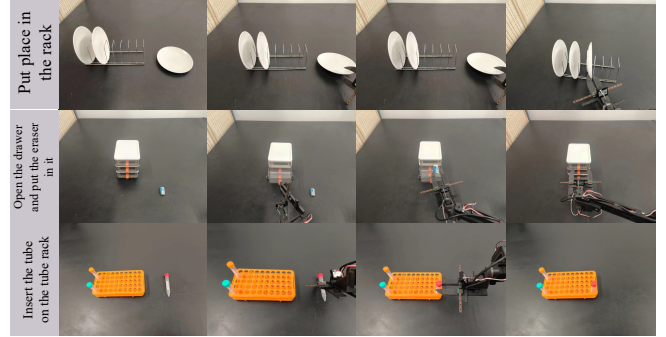


Fig. 7: **Teleoperation Tasks Demonstration.**

continuing until five sets of successful data were collected. We selected 3 tasks and recorded the success rate and the average time of successful attempts. The task examples and full results are shown in Fig. 7 and Table V.

The results demonstrate that, compared to baseline methods, our approach reduces completion time by an average of 30%, primarily due to its intuitive and simplified operation. In contrast, when using the SpaceMouse method, operators often became confused when switching between the main camera and the wrist camera for fine control, as the camera coordinate system changes while the teleoperator’s reference frame remains static, which increases operation time. Meanwhile, the incremental operation of the 3D mouse may result in a “dead zone” in certain tasks, such as the lower success

TABLE IV: Success Rate of Imitation Learning Tasks

Task Name	Pick Box	Insert Pen			Collect Toy		
		Pick up the Pen	Grasp the Cup	Insert the Pen	Pick up the Toy	Move to the Table	Stow in the Box
Success Rate	10/10	10/10	6/10	6/10	8/10	7/10	7/10

 TABLE V: Task Performance Comparison across Different Methods. **SR:** success rate. **Time:** average success time (s).

Task Name	RoboPilot		SpaceMouse		Leader-Follower	
	SR	Time	SR	Time	SR	Time
Put plate in the rack	100%	36.62	44.4%	47.31	100%	57.35
Open drawer and put the eraser in it	100%	72.60	100%	83.95	100%	82.69
Insert the tube on the tube rack	100%	26.44	100%	44.87	100%	55.94
Average	100%	45.22	81.5%	58.71	100%	65.33

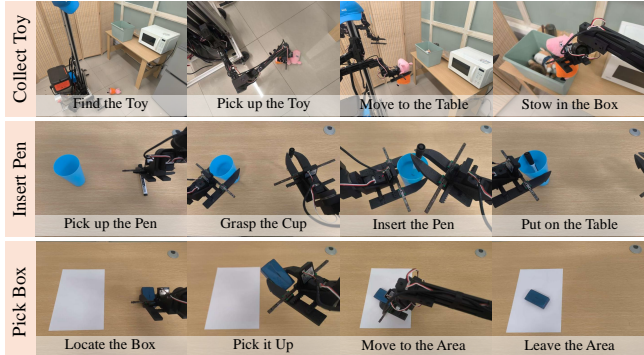


Fig. 8: **Virtualization of Imitation Learning Tasks.** The tasks consist of multiple sub-task stages and require changes in height or bimanual coordination.

rate observed in Task 1. For the leader-follower method, the ball joints of the robotic arm frequently encountered singular positions, requiring manual intervention to restore operation, which consumed additional time.

#### B. Very Long-horizon Remote Teleoperation

We carefully designed several very long-horizon and complex tasks to evaluate the boundary of the robot’s operational performance in the teleoperation system. **Task 1** involves a complete process of delivering coffee, requiring long-term teleoperation, full-body mobility, and precise environmental interactions. **Task 2** involves picking and heating food, requiring a large operational space (e.g., opening a microwave) and vertical mobility (the sushi is located in the lower part of a refrigerator, and the target location is on an upper-level table). Since Mobile Aloha lacks vertical movement capabilities, it is unable to complete Task 2. By using a web-based teleoperation interface over a cellular network, the operator was able to complete these tasks remotely. The visualizations are shown in Fig. 6, and the videos are available on the website.

#### C. Autonomous Task Execution via Imitation Learning

We conducted imitation learning experiments for AhaRobot on three sequential tasks, with task definitions provided in Fig. 8. The robot’s state was represented by

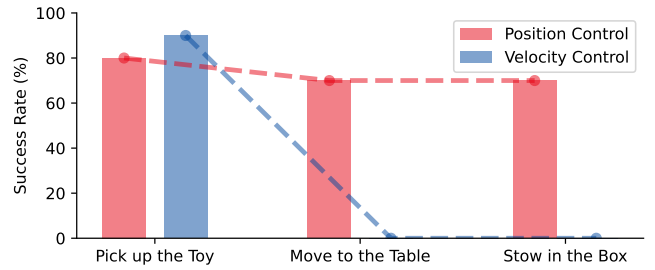


Fig. 9: **Success Rate of Different Types of Base Movement.** Due to spikes in the data, the policy trained by velocity control failed to move.

18 dimensions, including arm joint positions, gripper state, rotation angle of head camera, base movement command, and three images captured from the head and wrist cameras. Correspondingly, the teleoperator provided 18-dimensional commands through inverse kinematics. We collected 50 demos for the tasks “Pick Box” and “Insert Pen” and 80 demos for the task “Collect Toy” and trained the imitation learning model using the ACT [9] algorithm.

As shown in Table IV, each task was tested 10 times. Simple tabletop tasks such as “Pick Box” achieved a success rate of 100%. However, for the “Insert Pen” task, the lightweight nature of the cup made it prone to being knocked over, leading to out-of-distribution states and a performance drop in the “Grasp the Cup” step. For the whole-body task “Collect Toy”, the robot exhibited high inertia and low encoder resolution, requiring fine adjustments of its whole-body position using pedals. These factors caused spikes in the base velocity distribution during data collection. Therefore, we used position control for learning base movements instead of velocity control, achieving stable learning performance. We further compared different base movement control methods in Fig. 9 and demonstrated that position control allows easier and more stable learning of base movements.

## VII. CONCLUSIONS

In summary, we introduce AhaRobot, a cost-effective yet high-performance robot. We make innovative designs in three aspects: robot hardware configuration, control system

optimization, and whole-body teleoperation (RoboPilot), resulting in significant improvements in control accuracy and stability. AhaRobot can achieve complete remote teleoperation for long-horizon tasks and can autonomously complete complex tasks through imitation learning. The total budget for AhaRobot is only \$1000-2000, and it is fully open-source in both software and hardware, making it suitable for low-cost practical applications and research setups. However, AhaRobot still has some limitations. The AhaRobot embodiment is heavy and lacks collision sensing. And vision-based RoboPilot teleoperation inevitably suffers from transmission delays, making it difficult to operate highly dynamic and extremely complex tasks. Stronger software optimization can mitigate this issue. We hope that low-cost practical robotic equipment and solutions can promote the equality and sharing of embodied AI, advancing the widespread application of embodied robots in daily life.

## REFERENCES

- [1] T. Z. Zhao, V. Kumar, S. Levine, and C. Finn, “Learning fine-grained bimanual manipulation with low-cost hardware,” in *RSS*, 2023.
- [2] C. Chi, S. Feng, Y. Du, Z. Xu, E. Cousineau, B. C. Burchfiel, and S. Song, “Diffusion policy: Visuomotor policy learning via action diffusion,” in *RSS*, 2023.
- [3] M. J. Kim, K. Pertsch, S. Karamcheti, T. Xiao, A. Balakrishna, S. Nair, R. Rafailov, E. P. Foster, P. R. Sanketi, Q. Vuong, T. Kollar, B. Burchfiel, R. Tedrake, D. Sadigh, S. Levine, P. Liang, and C. Finn, “Openvla: An open-source vision-language-action model,” in *CoRL*, 2025.
- [4] O. team, “Octo: An open-source generalist robot policy,” in *RSS*, 2024.
- [5] S. Liu, L. Wu, B. Li, H. Tan, H. Chen, Z. Wang, K. Xu, H. Su, and J. Zhu, “Rdt-1b: A diffusion foundation model for bimanual manipulation,” in *ICLR*, 2025.
- [6] P. Liu, Y. Orru, J. Vakil, C. Paxton, N. M. M. Shafiullah, and L. Pinto, “Demonstrating ok-robot: What really matters in integrating open-knowledge models for robotics,” in *RSS*, 2024.
- [7] J. Zhang, K. Wang, R. Xu, G. Zhou, Y. Hong, X. Fang, Q. Wu, Z. Zhang, and H. Wang, “Navid: Video-based vlm plans the next step for vision-and-language navigation,” in *RSS*, 2024.
- [8] G. Zhou, Y. Hong, Z. Wang, X. E. Wang, and Q. Wu, “Navgpt-2: Unleashing navigational reasoning capability for large vision-language models,” in *ECCV*, 2025.
- [9] Z. Fu, T. Z. Zhao, and C. Finn, “Mobile aloha: Learning bimanual mobile manipulation using low-cost whole-body teleoperation,” in *CoRL*, 2024.
- [10] D. Honerkamp, H. Mahesheka, J. O. von Hartz, T. Welschehold, and A. Valada, “Whole-body teleoperation for mobile manipulation at zero added cost,” *IEEE Robotics and Automation Letters*, 2025.
- [11] X. Cheng, J. Li, S. Yang, G. Yang, and X. Wang, “Open-television: Teleoperation with immersive active visual feedback,” in *CoRL*, 2024.
- [12] R. Ding, Y. Qin, J. Zhu, C. Jia, S. Yang, R. Yang, X. Qi, and X. Wang, “Bunny-visionpro: Real-time bimanual dexterous teleoperation for imitation learning,” *arXiv:2407.03162*, 2024.
- [13] T. He, Z. Luo, X. He, W. Xiao, C. Zhang, W. Zhang, K. M. Kitani, C. Liu, and G. Shi, “Omnih2o: Universal and dexterous human-to-humanoid whole-body teleoperation and learning,” in *CoRL*, 2024.
- [14] J. Luo, C. Xu, J. Wu, and S. Levine, “Precise and dexterous robotic manipulation via human-in-the-loop reinforcement learning,” *arxiv:2410.21845*, 2024.
- [15] P. Wu, F. Shentu, X. Lin, and P. Abbeel, “Gello: A general, low-cost, and intuitive teleoperation framework for robot manipulators,” in *CoRL*, 2023.
- [16] H. Fang, H.-S. Fang, Y. Wang, J. Ren, J. Chen, R. Zhang, W. Wang, and C. Lu, “Airexo: Low-cost exoskeletons for learning whole-arm manipulation in the wild,” in *ICRA*, 2024.
- [17] S. Yang, M. Liu, Y. Qin, R. Ding, J. Li, X. Cheng, R. Yang, S. Yi, and X. Wang, “Ace: A cross-platform and visual-exoskeletons system for low-cost dexterous teleoperation,” in *CoRL*, 2024.
- [18] K. Shaw, Y. Li, J. Yang, M. K. Srirama, R. Liu, H. Xiong, R. Mendonca, and D. Pathak, “Bimanual dexterity for complex tasks,” in *CoRL*, 2024.
- [19] C. C. Kemp, A. Edsinger, H. M. Clever, and B. Matulevich, “The design of stretch: A compact, lightweight mobile manipulator for indoor human environments,” in *ICRA*, 2022.
- [20] D. Team, “Droid: A large-scale in-the-wild robot manipulation dataset,” in *RSS*, 2024.
- [21] H. Xiong, R. Mendonca, K. Shaw, and D. Pathak, “Adaptive mobile manipulation for articulated objects in the open world,” *arXiv:2401.14403*, 2024.
- [22] M. Spahn, C. Pezzato, C. Salmi, R. Dekker, C. Wang, C. Pek, J. Kober, J. Alonso-Mora, C. H. Corbato, and M. Wisse, “Demonstrating adaptive mobile manipulation in retail environments,” in *RSS*, 2024.
- [23] Y. Peng, Z. Wang, Y. Zhang, S. Zhang, N. Cai, F. Wu, and M. Chen, “Revolutionizing battery disassembly: The design and implementation of a battery disassembly autonomous mobile manipulator robot(beam-1),” in *IROS*, 2024.
- [24] J. Wu, W. Chong, R. Holmberg, A. Prasad, Y. Gao, O. Khatib, S. Song, S. Rusinkiewicz, and J. Bohg, “Tidybot++: An open-source holonomic mobile manipulator for robot learning,” in *CoRL*, 2024.
- [25] S. Xie, C. Hu, D. Wang, J. Johnson, M. Bagavathiannan, and D. Song, “Coupled active perception and manipulation planning for a mobile manipulator in precision agriculture applications,” in *ICRA*, 2024.
- [26] Q. Li, Q. Meng, Y. Qin, J. Chen, X. Ding, and K. Xu, “Dynamic interaction control in legged mobile manipulators: A decoupled approach,” in *ICRA*, 2024.
- [27] M. Zhang, Y. Ma, T. Miki, and M. Hutter, “Learning to open and traverse doors with a legged manipulator,” in *CoRL*, 2024.
- [28] M. Bajracharya, J. Borders, D. Helmick, T. Kollar, M. Laskey, J. Leichty, J. Ma, U. Nagarajan, A. Ochiai, J. Petersen, K. Shankar, K. Stone, and Y. Takaoka, “A mobile manipulation system for one-shot teaching of complex tasks in homes,” in *ICRA*, 2020.
- [29] M. Bajracharya, J. Borders, R. Cheng, D. Helmick, L. Kaul, D. Kruse, J. Leichty, J. Ma, C. Matl, F. Michel, C. Papazov, J. Petersen, K. Shankar, and M. Tjersland, “Demonstrating mobile manipulation in the wild: A metrics-driven approach,” in *RSS*, 2023.
- [30] T. Smith, M. Rijal, C. Tatsch, R. M. Butts, J. Beard, R. T. Cook, A. Chu, J. Gross, and Y. Gu, “Design of stickbug: A six-armed precision pollination robot,” in *IROS*, 2024.
- [31] C. Lenz, M. Schwarz, A. Rochow, B. Pätzold, R. Memmesheimer, M. Schreiber, and S. Behnke, “Nimbrio wins ana avatar xprize immersive telepresence competition: Human-centric evaluation and lessons learned,” *International Journal of Social Robotics*, 2023.
- [32] N. A. Hansen, H. Su, and X. Wang, “Temporal difference learning for model predictive control,” in *ICML*, 2022.
- [33]  $\pi_0$  Team, “ $\pi_0$ : A vision-language-action flow model for general robot control,” *arXiv:2410.24164*, 2024.
- [34] A. Iyer, Z. Peng, Y. Dai, I. Guzey, S. Haldar, S. Chintala, and L. Pinto, “Open teach: A versatile teleoperation system for robotic manipulation,” in *CoRL*, 2024.
- [35] A. Setapen, M. Quinlan, and P. Stone, “Marionet: Motion acquisition for robots through iterative online evaluative training,” in *AAMAS*, 2010.
- [36] C. Stanton, A. Bogdanovich, and E. Ratanasena, “Teleoperation of a humanoid robot using full-body motion capture, example movements, and machine learning,” *Australasian Conference on Robotics and Automation*, 2012.
- [37] C. Chi, Z. Xu, C. Pan, E. Cousineau, B. Burchfiel, S. Feng, R. Tedrake, and S. Song, “Universal manipulation interface: In-the-wild robot teaching without in-the-wild robots,” in *RSS*, 2024.
- [38] Z. Wu, T. Wang, C. Guan, Z. Jia, S. Liang, H. Song, D. Qu, D. Wang, Z. Wang, N. Cao, Y. Ding, B. Zhao, and X. Li, “Fast-umi: A scalable and hardware-independent universal manipulation interface,” *arXiv:2409.19499*, 2024.
- [39] R. Pfeifer, M. Lungarella, and F. Iida, “Self-organization, embodiment, and biologically inspired robotics,” *Science*, 2007.
- [40] H. Olsson, K. J. Åström, C. Canudas de Wit, M. Gäfvert, and P. Lischinsky, “Friction models and friction compensation,” *European Journal of Control*, 1998.
- [41] E. Olson, “Apriltag: A robust and flexible visual fiducial system,” in *ICRA*, 2011.
- [42] G. Schweighofer and A. Pinz, “Robust pose estimation from a planar target,” *IEEE Transactions on Pattern Analysis and Machine Intelligence*, 2006.